High-resolution Compton cameras based on Si/CdTe double-sided strip detectors

Hirokazu Odaka[a], Yuto Ichinohe[a,b], Shin'ichiro Takeda[a], Taro Fukuyama[a,b], Koichi Hagino[a,b], Shinya Saito[a,b], Tamotsu Sato[a,b], Goro Sato[a], Shin Watanabe[a], Motohide Kokubun[a], Tadayuki Takahashi[a,b], Mitsutaka Yamaguchi[c], Takaaki Tanaka[d], Hiroyasu Tajima[e], Kazuhiro Nakazawa[b], Yasushi Fukazawa[f]

[a]*Department of High Energy Astrophysics, Institute of Space and Astronautical Science (ISAS), Japan Aerospace Exploration Agency (JAXA), 3-1-1 Yoshinodai, Chuo, Sagamihara, Kanagawa, 252-5210, Japan*
[b]*Department of Physics, Graduate School of Science, University of Tokyo, Hongo 7-3-1, Bunkyo, Tokyo, 113-0033, Japan*
[c]*Takasaki Advanced Radiation Research Institute, Japan Atomic Energy Agency (JAEA), 1233 Watanuki-machi, Takasaki, Gunma, 370-1292, Japan*
[d]*Kavli Institute for Particle Astrophysics and Cosmology, Stanford University, Stanford, CA, USA.*
[e]*Solar-Terrestrial Environment Laboratory, Nagoya University, Furo-cho, Chikusa, Nagoya, 464-8601, Japan*
[f]*Department of Physical Science, Hiroshima University, 1-3-1 Kagamiyama, Higashi-Hiroshima, Hiroshima, 739-8526, Japan*

Abstract

We have developed a new Compton camera based on silicon (Si) and cadmium telluride (CdTe) semiconductor double-sided strip detectors (DSDs). The camera consists of a 500-μm-thick Si-DSD and four layers of 750-μm-thick CdTe-DSDs all of which have common electrode configuration segmented into 128 strips on each side with pitches of 250 μm. In order to realize high angular resolution and to reduce size of the detector system, a stack of DSDs with short stack pitches of 4 mm is utilized to make the camera. Taking advantage of the excellent energy and position resolutions of the semiconductor devices, the camera achieves high angular resolutions of 4.5 degrees at 356 keV and 3.5 degrees at 662 keV. To obtain such high resolutions together with an acceptable detection efficiency, we demonstrate data reduction methods including energy calibration using Compton scattering continuum and depth sensing in the CdTe-DSD. We also discuss imaging capability of the camera and show simultaneous multi-energy imaging.

Key words: gamma-ray imaging, Compton camera, CdTe double-sided strip detector

1. Introduction

A Compton camera using high-resolution semiconductor detectors is a promising gamma-ray imaging spectrometer in the energy band from 100 keV up to 10 MeV, in which Compton scattering is dominant over other interactions of a photon with matter. In astrophysics, gamma rays in this energy band are important probes of energetic phenomena in the universe such as cosmic-ray acceleration and nucleosynthesis. In this field, the first Compton telescope in orbit, *COMPTEL* [1], provided pioneering results of the gamma-ray sky. The gamma-ray imaging technique is also useful for medical imaging, nondestructive inspection, and search for radioactive isotopes.

The authors have been developing Compton cameras based on advanced technologies of silicon (Si) and cadmium telluride (CdTe) semiconductor detectors with high energy and position resolutions [2, 3, 4]. Adoption of such devices are great advantage to the angular (spatial) resolution since it depends mainly on precision of the energy and position measurements. Si is good scatterer since it yields a large Compton-scattering probability and has a small Doppler broadening effect; this effect degrades the angular resolution due to nonzero momentum of the target electron [5]. On the other hand, CdTe is used as absorber owing to its large photoelectric-absorption cross section. Using our camera prototypes [6], we have achieved an excellent angular resolution of 2.5 degrees at 511 keV [7], and have demonstrated high-resolution Compton imaging for diffuse emission as well as point sources, resolving a-few-millimeter scale structure at a distance of several centimeters from the detector head [8]. In addition, high-precision polarimetry was conducted using a synchrotron photon beam [9].

In this work, we have developed a new Compton camera that simultaneously realizes high angular resolution and compactness of the entire detector size. The high-density integration of the camera is essential to obtain acceptable detection efficiency for all applications and to achieve fine spatial resolution for near-source imaging such as medical applications. The camera consists of a compact multiple-layer stack of Si and CdTe double-sided strip detectors (DSDs) which have common geometrical configurations. This modular design allows us to optimize the scale (e.g. the number of the stacks) of the camera for future practical applications. In the present paper, we describe the detector design and analysis methods to obtain the high angular resolution with the ultra-compact instruments, and then show achieved performances. The detector concept is adopted as the key technology for the Hard X-ray Imager (HXI) and the Soft Gamma-ray Detector on board the *ASTRO-H* X-ray observatory, which is scheduled for launch in 2014 [10].

2. Detector design

The new Compton camera consists of a 500-μm-thick Si-DSD (collaboration with Hamamatsu Photonics) and four layers of 750-μm-thick CdTe-DSDs (collaboration with ACRORAD), as shown in Fig. 1. The CdTe detector holds aluminum

(Al) electrodes on the anode (high-voltage side) and platinum (Pt) electrodes on the cathode. As we adopt a modular design to assemble the detector system, the camera is designed as a stack of "standardized" detector trays with detector-to-detector pitches of 4 mm. Figure 2 shows the tray on which each detector is integrated with front-end readout electronics including eight signal processing ASICs (VATA 460). Each detector has the same active area of 32×32 mm^2 and the same electrode configuration that is segmented into 128 strips on each side with strip pitches of 250 μm. The readout ASIC simultaneously processes signals from 32 strips and digitizes the heights of the shaped pulses. The HXI onboard *ASTRO-H* adopts similar module, but it has different detector numbers (four Si-DSDs and one CdTe-DSD) and different readout ASICs (VATA 461).

In the experimental evaluation of the camera, these detectors were operated about −15°C. A bias of 250 V was applied to the Si-DSD for full depletion; a bias of 250 V was applied to the CdTe-DSDs, balancing between increasing charge collection efficiency and suppressing leakage currents. The typical energy resolution of the Si-DSD was 2.3 keV (full width at half-maximum or FWHM) at 59.5 keV. The CdTe-DSD achieved energy resolutions of 3.8 keV (FWHM) at 81.0 keV and $\Delta E/E = 3\%$ (FWHM) at 511 keV. Since VATA 460 is low-gain or high-dynamic-range type, its spectral performance is modest comparing to an energy resolution of 1.7 keV at 59.5 keV obtained by an equaivalent CdTe-DSD with high-gain type VATA 461. Detailed description of CdTe-DSDs are given by Watanabe et al. (2009) and Ishikawa et al. (2010) [11, 12].

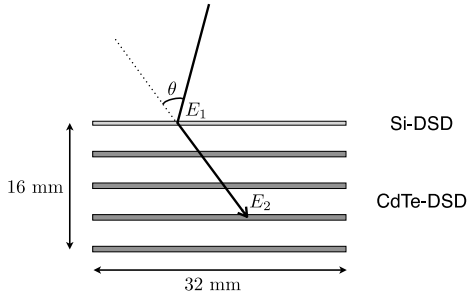

Figure 1: Schematic drawing of the Si/CdTe Compton camera.

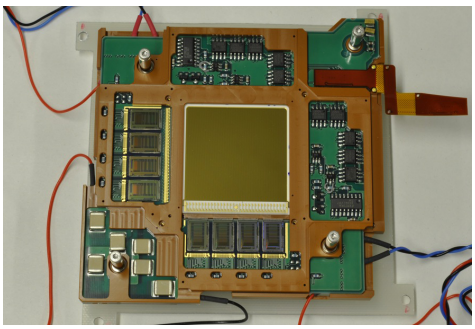

Figure 2: Photograph of the CdTe-DSD tray.

3. Data reconstruction

As shown in Fig. 1, a typical Compton event consists of a scattering in Si and an absorption in CdTe. By using the energies of the recoil electron (E_1) and of the scattered photon (E_2), the scattering angle θ_K and the energy E of the incident photon are given by the Compton kinematics,

$$\cos\theta_K = 1 - \frac{m_e c^2}{E_2} + \frac{m_e c^2}{E_1 + E_2}, \quad E = E_1 + E_2, \qquad (1)$$

where m_e is the electron mass and c is the speed of light. When the scattering angle θ_G is geometrically calculated by the positions of the two interactions and the given incident direction, the difference between the scattering angles calculated in two ways, $\Delta\theta = \theta_K - \theta_G$, provides the angular resolution measure (ARM) of the Compton camera. Obviously, uncertainties of the measured energies and positions affects the performance of Compton imaging. In this section, we describe analysis methods to fulfill simultaneously high angular resolution and sufficient efficiency.

3.1. Energy calibration

Accurate gain calibration are essential to make the best use of the high-resolution semiconductor detectors. Though we usually apply gamma-ray radioactive sources to energy calibration, it is not realistic to use photoelectric peaks at high energies for this purpose. Above 150 keV, photoelectric absorption hardly occurs in Si; furthermore, absorption events would be infrequent even in CdTe when the trigger logic requires event coincidence in both the Si and CdTe detectors.

We propose a calibration method using Si-CdTe two-hit events, which are major events of the Compton camera. The following is brief description of the calibration procedure. First, a temporary gain correction function from the pulse height value to the energy is determined by using photoelectric peaks below $E_{\rm sup} = 136$ keV (^{57}Co) for every readout channel. Above $E_{\rm sup}$, the functions are linearly extrapolated. At this step, we have obtained gain functions which are valid below $E_{\rm sup}$. Second, by using the two-hit events that satisfy $E_1 + E_2 = E_{\rm line}$ within a certain error and $E_1 < E_{\rm sup}$, we fit gain functions of the CdTe detectors represented as third-order polynomials, regarding a true value of E_2 as $E_{\rm line} - E_1$. Here, we have applied gamma-ray lines of 356 keV (^{133}Ba), 511 keV (^{22}Na), and 662 keV (^{137}Cs). Final gain correction functions of the CdTe detectors are obtained in the second step. Third, we fit gain functions of the Si detector above $E_{\rm sup}$, regarding a true value of E_1 as $E_{\rm line} - E_2$, where the calibrated values of E_2 at the second step are used. Consequently, we have obtained well-calibrated gain functions of all the detectors in the entire energy range.

Figure 3 shows correlations between E_1 (Si) and E_2 (CdTe) using the temporary gain functions at the first step and those at the final step for the ^{137}Cs data. After the calibration, the two-hit events are distributed along the line $E_1 + E_2 = E_{\rm line}$ (662 keV). This calibration method can be cross-checked by calibration test pulse input to the readout ASIC.

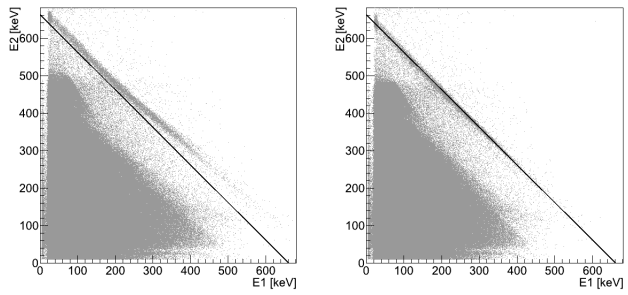

Figure 3: Correlations between E_1 (Si) and E_2 (CdTe) of ^{137}Cs data. The left panel uses the temporal gain function at the first calibration step; the right panel uses the final calibration functions. The lines $E_1 + E_2 = E_{\rm line}$ (662 keV) are superposed.

3.2. Event reconstruction and depth sensing

Before reconstruction of the scattered events, multiple signals in a DSD are reconstructed into a single hit. In the simplest case, a photon interaction generates two signals on one side and the other side. The hit position is determined as the intersection of the two strips, and the energy is taken from the P-side signal for the Si-DSD and from the Al-side signal for the CdTe-DSDs because these sides yield better spectral performance than the opposite sides. Since a charge-shared event, in which adjacent strips generate signals from a single photon hit, is not negligible for CdTe detectors[13], it is necessary to cluster such adjacent-strip signals. By clustering, we improve the detection efficiency of the 662 keV Compton events by a factor of 3.7 and that of the 356 keV Compton events by a factor of 1.7.

Depth sensing in the CdTe-DSD is an optional but interesting data reconstruction to improve the angular resolution. Due to the ineffective charge transport properties of holes in CdTe semiconductor and distorted weighting potential by small strip electrodes [14], the charge collection efficiency on the cathode (Pt-side) is significantly lower than that of anode (Al-side) (See Fig. 8 of Odaka et al. (2010) [15]). By utilizing this effect, we are able to estimate the interaction depth in the detector to improve the position resolution. In this work, we equally divided the 750-μm-thick CdTe detector into three volumes with thicknesses of 250 μm, which is equal to the strip pitch, and assigned the hit positions according to the ratio of the cathode-measuring energy to the anode-measuring energy.

After the hit reconstruction, we perform event reconstruction of a set of hits in multiple detectors. The object of the analysis is events that hit in Si once and CdTe once (two-hit events) and events that hit Si once and CdTe twice (three-hit events). An event including four or more hits is ineffective and negligible. For the two-hit events, we can safely assume that the Si hit is Compton scattering and the CdTe hit is absorption when the sum of the energies agrees with the line energy.

For the three-hit events, we determine the hit sequence as follows. The Si hit is regarded as the first Compton scattering, and the unsettled two CdTe hits should be ordered. Since fluorescence of CdTe (fluorescence yields ~0.5) can constitute the three-hit events, two hits in CdTe-DSDs that agree with energies of Kα or Kβ lines of Cd or Te are merged. Otherwise, there are two sequence possibilities: Si-CdTe1-CdTe2 or Si-CdTe2-CdTe1. Since the second interaction obeys the Compton kinematics and the positions of the first and second interactions give the incident direction, we can calculate $\Delta\theta$ of the second scattering for the two possibilities. We select the sequence that yields the smaller value of $\Delta\theta$, which is physically more consistent with the true sequence.

To check the correctness of the three-hit event analysis, Monte Carlo simulations were performed using the same detector setup for 662 keV photons. We selected three-hit events showing no escape from the camera, but eliminated events including a hit at the top CdTe detector because such events are contaminated by hits at the Si detector of photoelectron or fluorescence from CdTe. The simulation results show that the 95% of Si hits is generated via Compton scattering. In such events (including a Compton at Si), 61% is correctly sequenced, 23% contains a Si hit as the first Compton but wrong CdTe-hit order, and 16% contains a Si hit as the second Compton. The reconstruction accuracy of the three-hit events is 0.5-0.6, and this is acceptable for imaging applications because wrong events only contribute a pedestal level of the back-projection images.

4. Imaging performance

We evaluated the angular resolution of the Compton camera by measuring gamma-ray point sources located at a distance of 315 mm from the detector head. Figure 4 shows the ARM distribution at 662 keV (^{137}Cs). Event reconstruction was performed as described in §3, and the depth sensing analysis was also applied to assign the hit position in the CdTe-DSDs. To quantify the resolution, we fit the ARM distribution to a Voigt function (a convolution of a Lorentzian with a Gaussian function), and obtained its FWHM of 3.5 ± 0.1 degrees. Due to the well-calibrated energy scale, the ARM distribution does not display apparent systematic biases. In Figure 5, we extract a back-projection image of the cesium source from the same data of Fig. 4. The image shows the spatial resolution of 20 mm (FWHM) at a distance of 315 mm, being consistent with the angular resolution of 3.5°. At lower energy, the camera still has a high angular resolution of 4.5° at 356 keV (^{133}Ba).

Figure 6 shows the angular resolution as a function of the distance between the detectors of the first (Si) and second (CdTe) interactions for the 662 keV events, 356 keV events, and 662 keV events without the depth sensing analysis . We also show the contributions by the position uncertainty, which can be estimated by the detector position resolution [16], for two different depth resolutions in the CdTe-DSDs. The angular resolution improves with the distance between the two detectors because the angular uncertainty of the scattered photon direction gets smaller. Thus, the depth sensing analysis of the CdTe-DSD is particularly important for the top layer and promising approach to higher imaging performance. However, the experimental results show slight improvement probably because the depth accuracy is not sufficient and other contributions such as energy uncertainty and the Doppler broadening effects hide them.

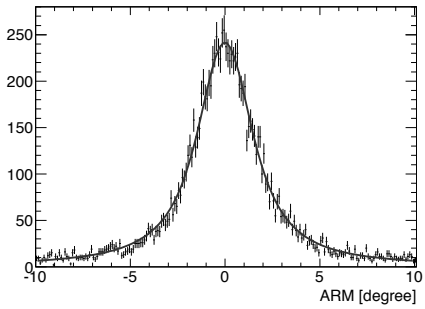

Figure 4: ARM distribution of ^{137}Cs 662 keV events. FWHM of the fitted Voigt function (solid line) is 3.5 ± 0.1 degrees.

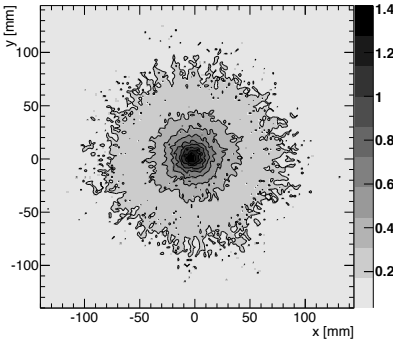

Figure 5: Back projection image of a point source of ^{137}Cs (662 keV) located at a distance of 315 mm. The image is presented in ten levels of grey linear scale with contours, showing a spatial resolution of 20 mm (FWHM).

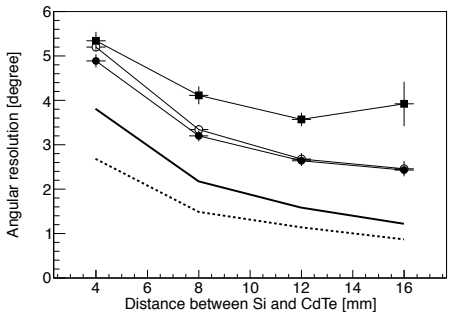

Figure 6: FWHMs of the ARM distributions for different event groups as functions of the distance between the Si detector of the first interaction and the CdTe detector of the second interaction. The top CdTe layer and the bottom CdTe layer correspond to values of 4 mm and 16 mm, respectively. The filled circles and filled squares shows the events of 662 keV and of 356 keV, respectively. The open circles are extracted from the events of 662 keV without the depth sensing analysis. The thick solid line represents estimated contributions of position uncertainties of detectors without depth resolution. The dotted line is similar estimation if the detector has depth resolution of 250 μm.

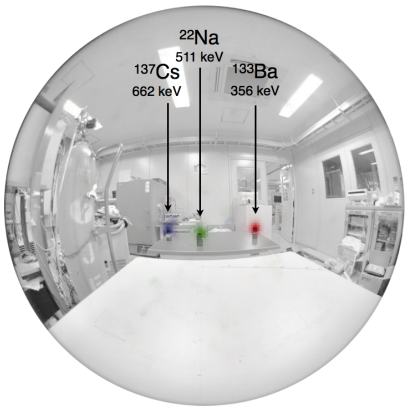

Figure 7: Energy-selected gamma-ray images extracted from the simultaneous measurements of three radioactive isotopes labeled in this figure. The distance to the sources from the camera is 1−1.3 m. The image is reconstructed by the LM-EM-ML method and translated to a combined fisheye picture with 180° field of view.

Finally, we demonstrate simultaneous multi-energy-source imaging using the Compton camera. We measured three different point sources, ^{133}Ba, ^{22}Na, and ^{137}Cs at the same time, and separately reconstructed Compton images by selecting the line energies. Figure 7 shows the gamma-ray images superposed on a 180° field-of-view fisheye picture of the laboratory. To make the image, a list-mode expectation-maximizing maximum-likelihood method [17, 8] is applied, and only a few hundred events are sufficient to reconstruct the point-like sources. This is advantage of the high resolution and recovers relatively low detection efficiency of 1.7×10^{-4} at 662 keV. Basic performance tests of this camera aimed at practical applications have been conducted by Takeda et al. [18].

References

[1] Schoenfelder, et al., Astron. Astrophys. Suppl. 120 (1996) 13.
[2] T. Takahashi, et al., SPIE, 4851 (2003) 1228.
[3] T. Tanaka, et al., Nucl. Instr. and Meth. A 568 (2006) 375.
[4] S. Watanabe et al., Nucl. Instr. and Meth. A 579 (2007) 871.
[5] A. Zoglauer, et al. Proc. SPIE 4851 (2003) 1302.
[6] S. Takeda, Ph. D. thesis, University of Tokyo (2008)
[7] S. Takeda et al., Proc. SPIE 6706 (2007) 67060S.
[8] S. Takeda et al., IEEE Trans. Nucl. Sci. 56 (2009) 783.
[9] S. Takeda et al., Nucl. Instr. and Meth. A 622 (2010) 619.
[10] T. Takahashi, Proc. SPIE 7732. (2010) 77320Z.
[11] S. Watanabe, et al., IEEE Trans. Nucl. Sci. 56 (2009) 777.
[12] S. Ishikawa, et al., JJAP 49, (2010) 116702
[13] G. Pellegrini, et al., IEEE Trans. Nucl. Sci. 53 (2006) 361.
[14] Z. He, Nucl. Instr. and Meth. A 463 (2001) 250.
[15] H. Odaka et al., Nucl. Instr. and Meth. A 624 (2010) 303.
[16] H. Odaka et al., Nucl. Instr. and Meth. A 579 (2007) 878.
[17] A. Zoglauer, Ph. D. thesis. (2005)
[18] S. Takeda, et al., submitted (2011)